Microarray analysis of senescent vascular smooth muscle cells: A link to atherosclerosis and vascular calcification

Dominick.G.A. Burton, Peter.J. Giles, Angela.N.P. Sheerin, S.Kaye Smith, Jessica.J. Lawton, Elizabeth.L. Ostler, William Rhys-Williams, David Kipling, Richard.G.A. Faragher

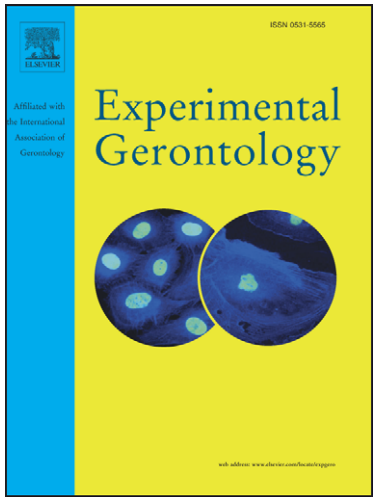

Microarray analysis of senescent vascular smooth muscle cells: A link to atherosclerosis and vascular calcification

Dominick.G.A. Burton, Peter.J. Giles, Angela.N.P. Sheerin, S.Kaye Smith, Jessica.J. Lawton, Elizabeth.L. Ostler, William Rhys-Williams, David Kipling, Richard.G.A. Faragher

PII: S0531-5565(09)00142-9
DOI: 10.1016/j.exger.2009.07.004
Reference: EXG 8628

To appear in: *Experimental Gerontology*

Received Date: 20 June 2009
Accepted Date: 18 July 2009

Please cite this article as: Burton, Dominick.G.A., Giles, Peter.J., Sheerin, Angela.N.P., Smith, S.Kaye, Lawton, Jessica.J., Ostler, Elizabeth.L., Rhys-Williams, W., Kipling, D., Faragher, Richard.G.A., Microarray analysis of senescent vascular smooth muscle cells: A link to atherosclerosis and vascular calcification, *Experimental Gerontology* (2009), doi: 10.1016/j.exger.2009.07.004

Running title: Microarray analysis of senescent vascular smooth muscle cells: A link to atherosclerosis and vascular calcification

Dominick G. A. Burton[1], Peter J. Giles[2], Angela N.P. Sheerin[1], S. Kaye Smith[2], Jessica J. Lawton[1], Elizabeth L. Ostler[1], William Rhys-Williams[3], David Kipling[2] , Richard G. A. Faragher*[1]

[1]School of Pharmacy & Biomolecular Science, University of Brighton, United Kingdom

[2]Department of Pathology, School of Medicine, Cardiff University, Heath Park, Cardiff CF14 4XN, United Kingdom

[3]Destiny Pharma Ltd, Science Park Square, Falmer, Brighton, United Kingdom

Correspondence

Richard G. A. Faragher, School of Pharmacy & Biomolecular Science, University of Brighton, UK. Tel: +44 (1273) 642124, Fax: +44 (273) 679333; email: rgaf@brighton.ac.uk

Key words: vascular calcification, atherosclerosis, cellular senescence, ageing, cardiovascular disease, vascular smooth muscle.

Abstract

Little is known about the senescent phenotype of human vascular smooth muscle cells (VSMCs) and the potential involvement of senescent VSMCs in age-related vascular disease, such as atherosclerosis. As such, VSMCs were grown and characterised *in vitro* to generate senescent VSMCs needed for microarray analysis (Affymetrix). Comparative analysis of the transcriptome profiles of early (14 CPD) and late (39-42 CPD) passage VSMCs found a total of 327 probesets called as differentially expressed: 149 are up-regulated in senescence and 178 repressed (*p*-value < 0.5%, minimum effect size of at least 2-fold differential regulation, explore data at www.madras.cf.ac.uk/vsmc). Data mining shows a differential regulation of genes at senescence associated with the development of atherosclerosis and vascular calcification. These included genes with roles in inflammation (IL1β, IL8, ICAM1, TNFAP3, ESM1 and CCL2), tissue remodelling (VEGF, VEGFβ, ADM and MMP14) and vascular calcification (MGP, BMP2, SPP1, OPG and DCN). The microarray data for IL1β, IL8 and MGP were validated by either, ELISA, Western blot analysis or RT-PCR. These data thus provide the first evidence for a role of VSMC senescence in the development of vascular calcification and provides further support for the involvement of senescent VSMCs in the progression of atherosclerosis.

Word count: 3800

1. Introduction

The ageing process represents a major challenge to current health care providers. Cardiovascular disease (CVD) accounts for approximately 56% of the total mortality in the over 65 age group and represents the single largest age-related cause of death (Brock *et al*, 1990, Mills *et al,* 1998). Atherosclerosis constitutes the single most important contributor to the increasing problem of CVD. A detailed understanding of the processes that contribute to the development and progression of atherosclerosis thus has important implications for the reduction of both mortality and morbidity in the elderly.

Cellular senescence is the irreversible growth arrest of mitotic cells, triggered by telomere shortening, oxidative stress or activated oncogenes (Serrano *et al* 1997, Bodnar *et al*, 1998, Rai *et al*, 2009). When a cell becomes senescent, it undergoes a substantial change in phenotype which is thought to predispose tissues to disease development. Many studies have investigated the potential role of cellular senescence in the development and progression of disease, including atherosclerosis (Burton, 2009, Erusalimsky, 2009). Senescence in endothelial progenitor cells (EPCs), vascular endothelial cells (VECs) and vascular smooth muscle cells (VSMCs) have all been implicated in the development and progression of atherosclerosis (Yang *et al*, 2008, Minamino *et al*, 2008, Matthews *et al*, 2006). However, the majority the of work on cellular senescence has been carried out on fibroblasts, with limited understanding of the phenotype of many other cell types, especially those linked to age-related pathology. As such, here we reported a detailed cell kinetic characterisation of the senescence of VSMCs followed by a transcriptome profile analysis, and we report changes of particular relevance to disease progression. Data on the proliferating, senescent and apoptotic fraction at each passage accompanies the analysed microarray data. This extends earlier studies reporting gene expression studies on senescence in other cell types, including fibroblasts, epithelial cells, endothelial cells and keratocytes (Shelton *et al* 1999, Chen *et al* 2004 and Kipling *et al*, 2009). Differences in the expression profiles of senescent

versus proliferating cells may provide insights into the potential role of senescent VSMCs cells in atherosclerosis.

2. Materials and methods

2.1 Cell culture

Human aortic smooth muscle cells were obtained from Cascade Biologics and grown in Medium 231 (Cascade Biologics) supplemented with smooth muscle growth supplement (Cascade Biologics) and penicillin (50u/L) and streptomycin (50µg/L). Cells were seeded at 5 x10^3 cells/cm^2 and sub-cultured every 5-10 days. Cells were cleaved using trypsin:EDTA and cell numbers determined by staining cells with trypan blue and counting live cells using a Bright line haemocytometer. For the measurement of the proliferating, senescent and apoptotic fractions of the culture at every passage, VSMCs were grown on 13mm diameter glass coverslips at identical seeding density to the parent culture. Prior to passage of parent culture, coverslips were harvested and processed as described below.

2.2 Growth kinetics of human vascular smooth muscle cells

2.2.1 Determination of the proliferating fraction

VSMCs grown on coverslips were washed and fixed in a 1:1 mixture of methanol:acetone for 5-10 minutes at room temperature. The fixed cells were then incubated for 1 hour at room temperature with a primary antibody raised against Ki67 (Dako M0722, mouse anti-Ki67, diluted in 1% (v/v) FCS in PBS, 1/20 dilution). The cells were then washed and incubated for a further hour in the dark at room temperature with a secondary antibody conjugated with FITC (Dako F0261, rabbit anti-mouse FITC, diluted using 1% (v/v) FCS in PBS, 1/20 dilution). Cells were washed and mounted using a DAPI based mountant (Vectorshield™) and viewed on a fluorescent microscope. Cycling cells show highly distinctive nuclear activity. To determine the proliferating

fraction, a total of 1000 cells were counted in random fields on each of three separate coverslips and the positive fraction determined.

2.2.2 Determination of senescence associated β-galactosidase activity

VSMCs grown on coverslips were washed and fixed in 4% paraformaldehyde for 10 minutes at room temperature. The fixed cells were washed and then incubated overnight at 37^{o}C in a solution of 4-chloro-5-bromo-3-indolyl-b-D-galactoside (X-Gal) in citric acid phosphate buffer containing 5mM potassium ferrocyanide and 5mM potassium ferricyanide (Dimri *et al*, 1995). To demonstrate the presence of β-galactosidase activity, one set of coverslips were incubated in buffer at pH 4; whilst to demonstrate senescence associated β-galactosidase (SA- β-gal), the incubation buffer was changed to pH 6. The cells were washed and counterstained using hematoxylin QS (Vector Labs) and nuclear fast red (Vector Labs) and viewed using a light microscope. To determine the senescent fraction, a total of 1000 cells were counted in random fields on 3 separate coverslips and the positive fraction determined.

2.2.3 Determination of apoptotic fraction

This was carried out using the Terminal Transferase mediated dUTP nick-end labelling (TUNEL) technique. Cells grown on coverslips were washed and fixed in 4% paraformaldehyde for 30 minutes at room temperature. Cells were washed and permeabilised with 0.1% Triton X100 for 2 minutes at 4^{o}C and then incubated for 1 hour at 37^{o}C with the reaction mixture (Roche) of terminal transferase and nucleotides including fluorescein-dUTP. Positive control cells were treated first with DNase I for 10 minutes at room temperature to induce double strand breaks prior to addition of the reaction mixture.

2.3 Microarray processing and analysis of gene expression

2.3.1 RNA isolation and microarray processing

Triplicate T75 tissue culture flasks containing VSMCs at ~80% confluence were used as the starting material for this analysis. Cells at 14 cumulative population doublings (CPD) were designated the growing population, those at a CPD range from 39-42 were used to generate 'senescent' RNA. Cell monolayers were rinsed briefly with phosphate-buffered saline and then lysed *in situ* using TRIzol (Invitrogen) as per the manufacturer's instructions. Total RNA quality was confirmed by spectrophotometry and by analysis on an Agilent 2100 Bioanalyser. 15µg of labelled cRNA was prepared, essentially as per the standard Affymetrix protocol, from 10µg of total RNA, using the Superscript II system (Invitrogen) and BioArray High Yield Kit (Enzo), and then hybridised to U133A GeneChips. (See MIAMEdata in Supplementary Material).

2.3.2 Microarray Data analysis

Expression values and Absent/Present calls were calculated using MAS 5.0 (Affymetrix, 2002) and RMA (Irizarry, 2003) expression summary algorithms, as implemented in R (version 2.3.1; R Development Core Team, 2005) within the Bioconductor simpleaffy (Wilson and Miller, 2005) and affy (Gautier, 2004) packages.

The U133A GeneChip carries 22,215 non-control probesets corresponding to over 13387 distinct human genes (that is, 13387 distinct Entrez Gene identifiers). Detection of differentially expressed genes was performed in three distinct separate ways. First, MAS 5.0 expression values were analysed using the Bayesian *t*-test approach implemented by Baldi and Long (2001) in the Cyber-t package. Second, RMA data was analysed by the Cyber-t approach. Third, RMA data was analysed using the limma package (Smyth, 2004). In each case we applied an addition filter requiring a minimum absolute fold change of at least 2 fold. Cyber-t and limma make use of moderated *t* statistics, which provides for greater power at small sample sizes as in this study. Multiple testing correction was performed using the False Discovery Rate (FDR) method (Benjamini and Hochberg, 1995) using a

common threshold of 0.5%. Enrichment analysis was performed using the Metacore analysis tool from GeneGo (Genego Inc, St Joseph, MI).

2.4 Validation of microarray data

2.4.1 Determination of cytokine concentration by Enzyme-Linked ImmunoSorbent Assay (ELISA)

VSMCs from early (14 CPD) and late (42 CPD) passage cultures were seeded (5000 cells/cm^2) into 24 well plates. Growth medium was collected from triplicate wells at 2, 4 and 6 hours and stored at -80ºC until use. Cells stimulated with bacterial LPS for the purpose of invoking a cytokine response were used as positive controls. Once the optimum protein dilutions were determined, ELISA was performed using a commercial kit in accordance with the manufactures instructions (R&D systems) on the diluted samples and known standards.

2.4.2 Western blot analysis

Whole-cell lysates from senescent and growing VSMCs were collected using TOTEX buffer with protease inhibitors. Protein lysates (based on equal cell number, rather than equal amounts of protein) were separated using SDS-PAGE and transferred to polyvinylidene fluoride (PVDF) membrane. Using optimised blocking conditions (milk powder) and antibody concentrations, the PVDF membrane(s) were placed in blocking buffer for 1 hour at room temperature on an orbital shaker. Membranes were then incubated with primary antibody in blocking buffer for a further hour at room temperature. The membranes were washed in PBS/Tween and then incubated with the appropriate secondary antibody with blocking buffer for 1 hour at room temperature followed by washing. The membranes were then incubated with the detection solution (ECL plus, Amersham Biosciences) for 5 minutes and exposed to either film or developed using a chemiluminescence imaging system (Alpha Innotech).

2.4.3 Reverse transcription-polymerase chain reaction (RT-PCR)

To validate the differential expression observed by microarray analysis, semi-quantitative RT-PCR was also used. RNA was extracted from early (15 CPD) and late (44 CPD) passage cultures of VSMCs according to the manufacturer's protocol (QIAGEN*).* This RNA (based on equal cell numbers rather than equal amounts of RNA) was used to generate and amplify cDNA. PCR products were electrophoresed on 1.5% agrose TAE gel containing ethidium bromide. GAPDH was used as a control. Quantification of the PCR products was accomplished by the use of a fluorchem imaging system (Alpha Innotech).

3. Results

3.1 Characterisation of senescence in human vascular smooth muscle cells

The VSMC culture used in this study proliferated for approximately 43 CPD before ceasing to expand any further (Figure 1A). As shown in Figure 1B, the culture initially showed a high fraction of Ki67 positive nuclei, which declined gradually with serial passage at a rate of decline of -1.29± 0.28 % Ki67 positive cells per population doubling.

The fraction of VSMCs senescence associated β-galactosidase activity (Dimri *et al*., 1995) throughout the lifespan of the culture is shown in Figure 1B. Less than 10% of cells stained positive until the last ten population doublings of the culture lifespan. The fraction of apoptotic (TUNEL positive) cells remained below 0.1% for most of the culture lifespan, but increased to ~1.3% in the last passage (Figure 1B).

3.2 Analysis of gene expression in senescent VSMCs

RNA samples were prepared from three independent replicates of early (14 CPD) and late (39-42 CPD) passage VSMC cultures and used for Affymetrix GeneChip expression analysis to compare the transcriptome profile of proliferating and senescent VSMCs.

Three different analytical methods were used to identify genes that were differentially regulated between early and late passage VSMCs. In each case a *p*-value threshold was selected at which < 0.5% of the resultant probeset list would be expected to be false positives. In addition, we also required a minimum effect size of at least 2-fold differential regulation. A total of 327 probesets were called as differentially expressed by all three methods and were chosen for further analysis; 149 are up-regulated in senescence and 178 repressed. Figure 2 is a MVA plot of the RMA data with the 327 probesets identified. A Venn diagram (Figure S1) detailing the derivation of this list of 327 probesets, a heatmap (Figure S2) of the MAS 5.0 data for the 327 probesets and a table (Table S1) of the RMA expression values (+/- SEM) for the 327 probesets are provided as Supplementary Material. This data can also be explored with a web-accessible and fully searchable public-access database (www.madras.cf.ac.uk/vsmc).

To focus more closely on disease processes, a manual review of the literature prior to commencement of data collection was undertaken with the aim of creating a genelist of known genes involved in the atherosclerotic or vascular calcification processes. From this search a list of 15 genes was generated (Table 1) which appear to have roles in either inflammation (IL1β, IL8, ICAM1, TNFAP3, ESM1 and CCL2) or tissue remodelling (VEGF, VEGFβ, ADM and MMP14). Genes involved in vascular calcification included: DCN, BMP2, SPP1, OPG and MGP. Of these 15 genes, all except SPP1 and ADM have at least one probeset that is also found in the 327 probeset list. Indeed, of the 30 probesets found in this disease list, 24 are present also in the 327 probeset list (see Supplemental Material). As shown in Table 1, with the exception of DCN, MGP and OPG, all the remaining genes are up-regulated in senescent VSMCs.

Enrichment analysis (EA) of the 149 probesets up-regulated at senescence and the 178 probesets repressed at senescence was performed using the Metacore analysis tool from GeneGo (Genego Inc, St Joseph, MI). Metacore is a database of known molecular interactions, pathways and processes manually curated from published data that enables the user to visualise known biological systems represented by their data. EA searches

for annotations that are significantly overrepresented within a given sample set. (see GeneGoEA in Supplementary Material).

Within the up-regulated 149 sample set, vascular disease was ranked number two in the top ten GeneGo diseases. Within the repressed 178 sample set, bone tissue neoplasms are ranked within the top ten GeneGo diseases.

3.3 Validation of microarray data

In order to validate the microarray data, Western blot, ELISA and RT-PCR was undertaken on the proinflammatory cytokines IL8 and IL1β, as well as matrix Gla protein (MGP).

Figure 3 shows semi-quantitative qRT-PCR for IL8 mRNA in early and late passage samples. The increase in IL8 mRNA that is seen by qRT-PCR is in qualitative agreement with the Affymetrix data. To further determine whether this difference in mRNA abundance results in differences in protein level, levels of IL8 in the medium of early and late passage cultures collected at 2, 4 and 6 hours after seeding were determined by ELISA (Figure 4). The result shows an increase in the concentration of IL8 protein in late passage samples compared with early passage samples (14 fold increase at two hours, 4 fold at four hours and 2.7 fold at six hours).

Although IL1β protein does not appear to be secreted by early or late passage VSMCs (data not shown), immunoblot analysis of IL1β of whole cell extracts revealed a strong signal in late passage samples, with no detectable IL1β in early passage VSMCs (Figure 5). It has been reported previously that in VSMCs, IL1 is not processed into its mature 17 KDa form and thus not secreted (Schonbeck *et al*, 1997). VSMCs express IL1α and IL1β as 33KDa precursor proteins, which do not contain a hydrophobic leader sequence needed for secretion. Western blot analysis of IL1β confirmed these findings and presented a band at the same size of the unprocessed form of IL1β (Figure 5). This unprocessed membrane bound form of IL1 has been shown to be functionally active (Loppnow and Libby, 1992).

Finally, the elevated mRNA for MGP seen by Affymetrix analysis in senescent VSMCs was validated by qRT-PCR (Figure 3), which revealed an approximately 7.5 fold decrease in MGP transcript abundance in the late passage sample compared the early passage sample.

4. Discussion

Senescence of VSMCs has been previously demonstrated using cultures derived from the rabbit (van der Loo *et al.* 1998) but to our knowledge this is the first report in which the kinetics of senescence in human VSMCs has been quantified. These data show that VSMCs undergo a clear process of senescence *in vitro* (Figure 1B). As with several other human cell types (including fibroblasts, mesothelial cells, retinal pigmented epithelial cells and vascular endothelium) the proliferating fraction of VSMCs decreases gradually rather than undergoing a rapid collapse at the end of the culture lifespan. This gradual decline in the proliferating fraction of VSMCs is probably associated with telomere shortening, resulting in an increasing likelihood of a cell becoming senescent with each serial passage. Evidence for telomere shortening in VSMCs has been provided by Matthews *et al* (2006), who also showed that telomere shortening in VSMCs was closely associated with increasing severity of atherosclerosis.

The gradual decline in the growth fraction is not mirrored by the expected gradual increase in the senescent fraction (as measured by senescence associated β-galactosidase (SA-β-Gal) staining) which instead shows an abrupt non-linear increase (Figure 1B). A similar observation has been made previously using human mesothelial cells (Thomas *et al*. 1997). This abrupt increase in the senescent fraction may be related to the indirect nature of the β-galactosidase assay technique, which measures lysosomal mass (and cell size) rather than growth state (Lee *et al.* 2006). Although large cell size correlates with senescence in many cell types, it is known that not all senescent cells within a given culture are large (Mitsui *et al.* 1981). Thus the SA-β-Gal assay almost certainly underestimates the number of senescent cells present in a given sample (Burton *et al*, 2007). This needs to be borne

in mind when the assay is used in morphometric estimates of 'senescent' cell number.

The data also demonstrated that baseline apoptosis rates do not alter significantly in VSMCs as the fraction of senescent cells within the culture increases (Figure 1B). This finding is in agreement with both the observations of Fenton *et al* (2001) on rabbit neointima *in vivo* and data from Clark and co-workers (Norsgaard *et al.* 1996), who found no difference in apoptosis rates between senescent and growing keratinocytes. This implies that senescent VSMCs may persist *in vivo* long enough to be of physiological significance in the pathogenesis of vascular disease. However, it has been reported that apoptosis is a feature of advanced atherosclerosis and this could promote telomere shortening (and thus senescence) by reducing the number VSMCs capable of replication (Matthews et al, 2006). Apoptosis in this instance is likely related to disease specific changes, such as an increase in oxidative stress, which is not normally observed during cell culture. Therefore, in addition to understanding the growth kinetics of VSMCs *in vitro*, it is also important to have insight into factors associated with disease, which could disrupt these kinetics *in vivo*.

Cellular senescence of endothelial progenitor cells (EPCs), vascular endothelial cells (VECs) and vascular smooth muscle cells (VSMCs) have all been suggested to have causal roles in the development of atherosclerosis (Yang et al, 2008, Minamino et al, 2008, Matthews et al, 2006). This may be due to an impaired ability to replace damaged/lost cells due to senescent EPCs, the reduced proliferative capacity of these tissues owing to the presence of senescent cells, the altered cellular phenotype of the senescent cells, the changed tissue microenvironment of the artery due to the different spectrum of proteins secreted by senescent cells, or a combination of all four. To provide further insight into the potential mechanisms whereby senescent VSMCs might contribute to age-related pathology, we undertook Affymetrix GeneChip expression analysis to compare the gene expression profile of proliferating versus senescent VSMCs.

A total of 327 probesets were called as differentially expressed in senescent VSMCs by all three of the analytical methods used (Figure S1) (p-value < 0.5%, > 2 fold change): 149 are up-regulated in senescence and 178

repressed. Almost all the genes that we defined in advance from the literature as being potentially involved in vascular pathologies are found within the 327 probesets differentially regulated in senescent VSMCs (Table 1). These differentially regulated genes have roles in inflammation, tissue remodelling or calcification and constitute less than 1.5% of all the probesets on the HG-U133A microarray. These include genes that are both up- and down-regulated in senescence. In addition to this, enrichment analysis (EA) of the 149 transcripts up-regulated in senescent VSMCs, ranked "vascular disease" at number two within the top ten GeneGo diseases. EA of the 178 repressed probesets in senescent VSMCs also provided links to calcification, with "bone tissue neoplasms" being present within the top ten GeneGo diseases. This thus suggests a strong link between the senescent transcriptome and age-related vascular disease.

A number of key genes known to be up-regulated in atherosclerotic plaques are also highly up-regulated in senescent VSMCs. These include IL-1β (validated by Western blot analysis, Figure 5), IL-8 (validated by ELISA, Figure 4) and ICAM-1, which are all involved in plaque formation. Cultures of smooth muscle cells (SMC) derived from plaques have been reported to show a reduced proliferative capacity (Bennett *et al* 1995) so it is not unreasonable to suggest that messages typically thought of as characteristic of plaque may in fact come from the senescent cells within the population. It is provocative in this regard that the experimental induction of oncogene-induced senescence (OIS) in rat smooth muscle *in vivo* produces a very similar increase in pro-inflammatory cytokines (including IL-1β and IL-8) to that which we observe *in vitro* (Minamino *et al.* 2003).

We have also demonstrated for the first time that senescent VSMCs adopt a phenotype that has the potential to predispose vascular tissue to calcification, leading to reduced elasticity and compliance. The mechanism underlying vascular calcification is currently unknown. However, a number of studies have suggested that the process of vascular calcification is similar to the mineralisation process observed in bone (Abedin *et al*, 2004).

Transcription of matrix Gla protein (MGP), an inhibitor of calcification is repressed in senescent VSMCs (validated by RT-PCR, Figure 4), while the transcript encoding bone morphogenic protein 2 (BMP2), a promoter of

calcification is up-regulated (~3-fold) in senescent VSMCs. Other genes associated with calcification which are also differentially regulated in senescent VSMCs include osteopontin, osteoprotegerin and decorin. In addition to this, EA of the 178 repressed probesets in senescent VSMCs found “bone tissue neoplasms” to be present within the top ten GeneGo diseases. Bone tissue neoplasms do not refer to neoplasms located in bones, but to normal or soft tissue which have become ossified (bony tissue). Thus, the appearance of calcification, a common feature of advanced atherosclerotic plaques may be due to the appearance of senescent VSMCs with their pro-calcificatory phenotype. Interestingly, Tyson *et al* have shown that VSMCs appear to be important in vascular calcification, since VSMCs within calcified plaques have been shown to express osteoblast and chondrocyte-like gene expression profiles (Tyson et al, 2003). Therefore, it is not unreasonable to suggest that the observed VSMCs within calcified plaques in this instance, may in fact be senescent VSMCs.

These findings provide a strong link between the senescent phenotype of VSMCs and a potential involvement in the progression of atherosclerosis and the development of vascular calcification. The pro-inflammatory and tissue-degrading phenotype of VSMC is not a surprising one, as it appears to be a common feature of the senescent phenotype in multiple cell types, but is not necessarily a universal characteristic (Kipling *et al*, 2009). It was surprising however to see senescent VSMCs adopt a pro-calcificatory phenotype. This observation suggests the need to understand cell-type specific changes which may occur during cellular senescence. An understanding of such changes would provide further insight into the relationship between cellular senescence and ageing/age-related diseases.

Acknowledgments

Kaye Smith and Angela Sheerin were supported by the Biotechnology and Biological Sciences Research Council (EGH16151, EGH16152). Peter J. Giles was supported by the Wales Gene Park.

References

Abedin, M., Tintut, Y., and Demer, L. L. (2004). Vascular calcification: mechanisms and clinical ramifications. Arterioscler Thromb Vasc Biol *24*, 1161-1170.

Affymetrix (2002) Statistical Algorithms Description Document. Affymetrix, Inc, Santa Clara, CA.

Baldi, P. and Long, A.D. (2001) A Bayesian framework for the analysis of microarray expression data: regularized t -test and statistical inferences of gene changes, Bioinformatics 17:509-519.

Benjamini, Y., Hochberg, Y. (1995) Controlling the false discovery rate: a practical and powerful approach to multiple testing, J R Stat Soc 57:289-300

Bennet MR, Evan GI, Schwartz SM (1995) Apoptosis of human vascular smooth muscle cells derived from normal vessels and coronary atherosclerotic plaques. J. Clin Invest 95: 2266-2274.

Bodnar AG, Ouellette M, Frolkis M, Holt SE, Chiu CP, Morin GB, Harley CB, Shay JW, Lichtsteiner S, Wright WE. (1998). Extension of life-span by introduction of telomerase into normal human cells. Science. Jan 16;279(5349):349-52

Brock DB, Guralnik JM, Brody JA: Demography and epidemiology of aging in the United States, in Schneider E (Ed): Handbook of the biology of aging, Third Edition. Academic Press Inc. (1990) p3.

Burton, DGA, Sheerin, A, Ostler, E.L, Smith, K, Giles, P.J, Lowe, J, Rhys-Williams, W, Kipling, D.G and Faragher, R.G.A (2007) Cyclin D1 over-expression permits the reproducible detection of senescent human vascular smooth muscle cells. Ann N Y Acad Sci. 2007 Nov;1119:20-31

Burton DGA (2009) Senescence, Ageing and Disease. Age (Dordr). 2009 Mar;31(1):1-9

Chen, H. L., Lu, C. Y., Hsu, Y. H., and Lin, J. J. (2004). Chromosome positional effects of gene expressions after cellular senescence. Biochem Biophys Res Commun *313*, 576-586.

Dimri, G, Lee, X, Basile G, Acosta, M, Scott, G, Roskelly, C, Medrano, EE, Linskens, M, Rubelj, I, Periera-Smith, OM, Peacocke, M, Campisi J. A biomarker that identifies senescent human cells in culture and in aging skin *in vivo*. *Proc Natl Acad Sci* 1995; 92**:** 9362-9367

Erusalimsky J.D (2009) Vascular endothelial senescence: from mechanisms to pathophysiology. J Appl Physiol. Jan;106(1):326-32.

Fenton M, Barker S., Kurz D.J., Erusalimsky J.D. (2001) Cellular senescence after single and repeated catheter denudations of rabbit carotid arteries. Arterioscler. Thromb. Vasc. Biol. 21:220-226

Gautier, L., Cope, L., Bolstad, B.M., Irizarry, R.A. (2004) affy-analysis of Affymetrix GeneChip data at the probe level. Bioinformatics, 20:307-15

Irizarry, R.A., Hobbs, B., Collin, F., Beazer-Barclay, Y.D., Antonellis, K.J., Scherf, U. and Speed, T.P. (2003) Exploration, normalization, and summaries of high density oligonucleotide array probe level data. Biostatistics, 4:249-264.

Kipling D, Jones DL, Smith SK, Giles PJ, Jennert-Burston K, Ibrahim B, Sheerin AN, Evans AJ, Rhys-Willams W, Faragher RG. (2009) A transcriptomic analysis of the EK1.Br strain of human fibroblastoid keratocytes: the effects of growth, quiescence and senescence. Exp Eye Res. Feb;88(2):277-85

Lee BY, Han JA, Im JS, Morrone A, Johung K, Goodwin EC, Kleijer WJ, DiMaio D, Hwang ES (2006) Senescence-associated □ galactosidase is lysosomal □ galactosidase. Aging Cell 5: 187-197.

Loppnow, H., and Libby, P. (1992). Functional significance of human vascular smooth muscle cell-derived interleukin 1 in paracrine and autocrine regulation pathways. Exp Cell Res *198*, 283-290.

Matthews C, Gorenne I, Scott S, Figg N, Kirkpatrick P, Ritchie A, Goddard M, Bennett M. (2006) Vascular smooth muscle cells undergo telomere-based senescence in human atherosclerosis: effects of telomerase and oxidative stress. Circ Res. Jul 21;99(2):156-64

Mills E (Chair) (1998) Prevention of dependency in later life study group.:Continuing Care Conference: Fit for the future: The prevention of dependency in later life. Edited by Helen Prophet. Published by: Continuing Care Conference.

Minamino T, Yoshida T, Tatento K, Miyauchi H, Zou Y, Toko H, Komouro I (2003) Ras induces vascular smooth muscle cells senescence and inflammation in human atherosclerosis. *Circulation* 108:2264-2269.

Minamino T, Komuro I (2008) Vascular aging: insights from studies on cellular senescence, stem cell aging, and progeroid syndromes. Nat Clin Pract Cardiovasc Med. 2008 Oct;5(10):637-48

Mitsui Y, Smith JR, Schneider EL. J. Gerontol 1981 Jul;36(4):416-9
Equivalent proliferation potential different size classes of human diploid fibroblasts.

Norsgaard H, Clark BF, Rattan SI (1996) Distinction between differentiation and senescence and the absence of increased apoptosis in human

keratinocytes undergoing cellular aging in vitro. Exp Gerontol. 1996 Sep-Oct;31(5):563-70

Rai P, Onder TT, Young JJ, McFaline JL, Pang B, Dedon PC, Weinberg RA. (2009) Continuous elimination of oxidized nucleotides is necessary to prevent rapid onset of cellular senescence. Proc Natl Acad Sci U S A. Jan 6;106(1):169-74

Schonbeck, U., Herzberg, M., Petersen, A., Wohlenberg, C., Gerdes, J., Flad, H. D., and Loppnow, H. (1997). Human vascular smooth muscle cells express interleukin-1beta-converting enzyme (ICE), but inhibit processing of the interleukin-1beta precursor by ICE. J Exp Med *185*, 1287-1294.

Serrano M, Lin AW, McCurrach ME, Beach D, Lowe SW (1997) Oncogenic ras provokes premature cell senescence associated with accumulation of p53 and p16INK4a. Cell. Mar 7;88(5):593-602

Shelton DN, Chang E, Whittier PS, Choi D, Funk WD. Microarray analysis of replicative senescence. *Curr Biol* 1999; 9: 939-945

Smyth GK (2004) Linear models and empirical bayes methods for assessing differential expression in microarray experiments. Stat Appl Genet Mol Biol. 2004;3:Article3

Thomas E, Al-Baker E, Dropcova S, Denyer S, Ostad N, Lloyd A, Kill IR, Faragher RGA: Different kinetics of senescence in human fibroblasts and peritoneal mesothelial cells. Exp Cell Res 236: 355, 1997.

Tyson, K. L., Reynolds, J. L., McNair, R., Zhang, Q., Weissberg, P. L., and Shanahan, C. M.(2003). Osteo/chondrocytic transcription factors and their target genes exhibit distinct patterns of expression in human arterial calcification. Arterioscler Thromb Vasc Biol *23*, 489-494.

Van der Loo B, Fenton MJ, Erusalimsky JD (1998) Cytochemical detection of a senescence associated galactosidase in endothelial and smooth muscle cells from human and rabbit blood vessels. Exp Cell Res 241: 309-315.

Wilson, C.L., Miller, C.J. (2005) Simpleaffy: a BioConductor package for Affymetrix Quality Control and data analysis, Bioinformatics 21:3683-5

Yang DG, Liu L, Zheng XY. (2008) Cyclin-dependent kinase inhibitor p16(INK4a) and telomerase may co-modulate endothelial progenitor cells senescence. Ageing Res Rev. 2008 Apr;7(2):137-46

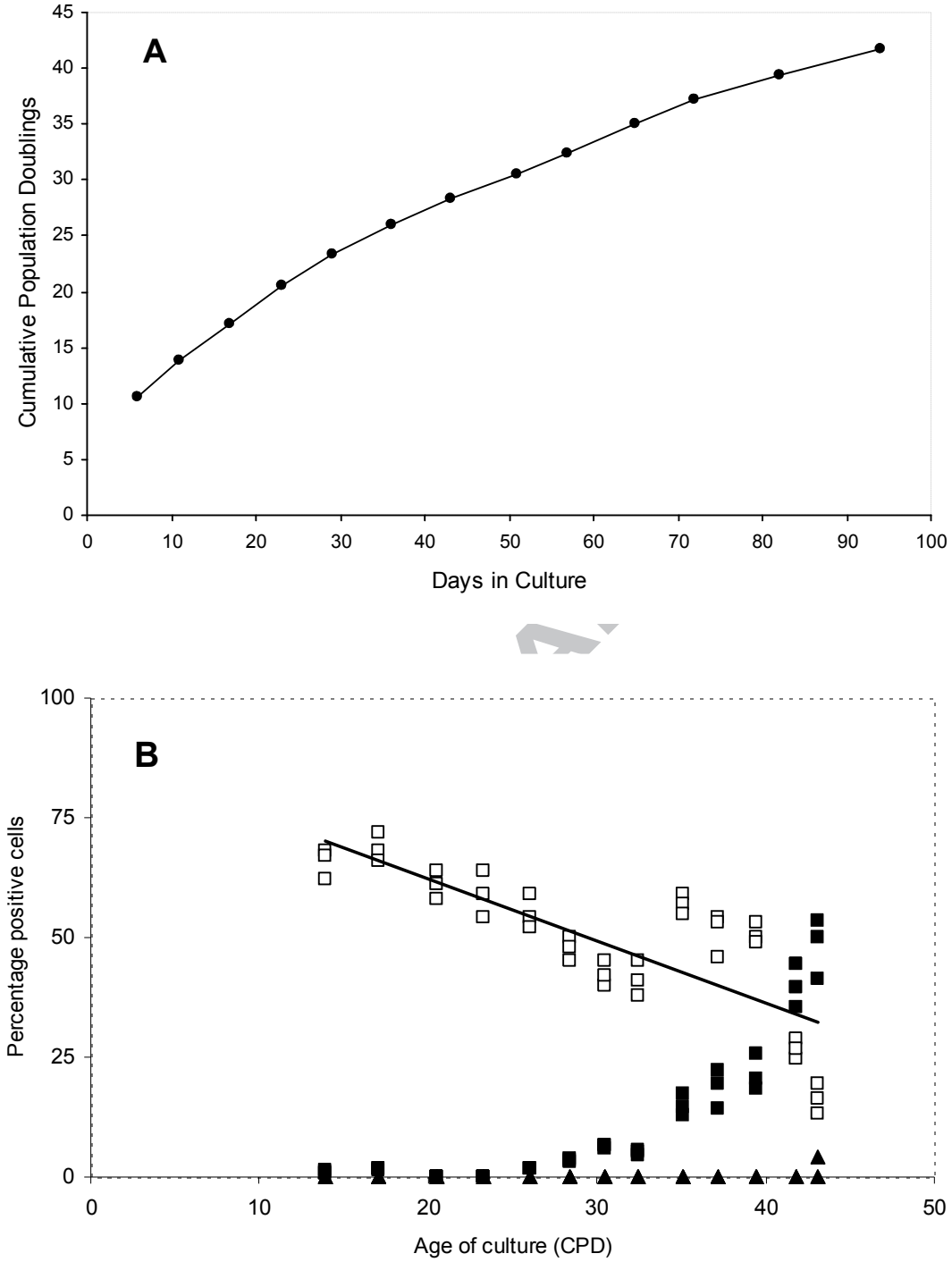

Figure 1: (A) Growth curve for VSMCs, (B) Growth Kinetics of VSMCs. Rate of decline in the cycling fraction of VSMCs (open squares) visualised by staining for the proliferation marker Ki67. Data are fitted to simple linear regression. Rate of increase in the senescent fraction (solid squares) as measured by SA-β-Gal assay. Apoptotic fraction of VSMCs (solid triangles) visualised using the TUNEL assay.

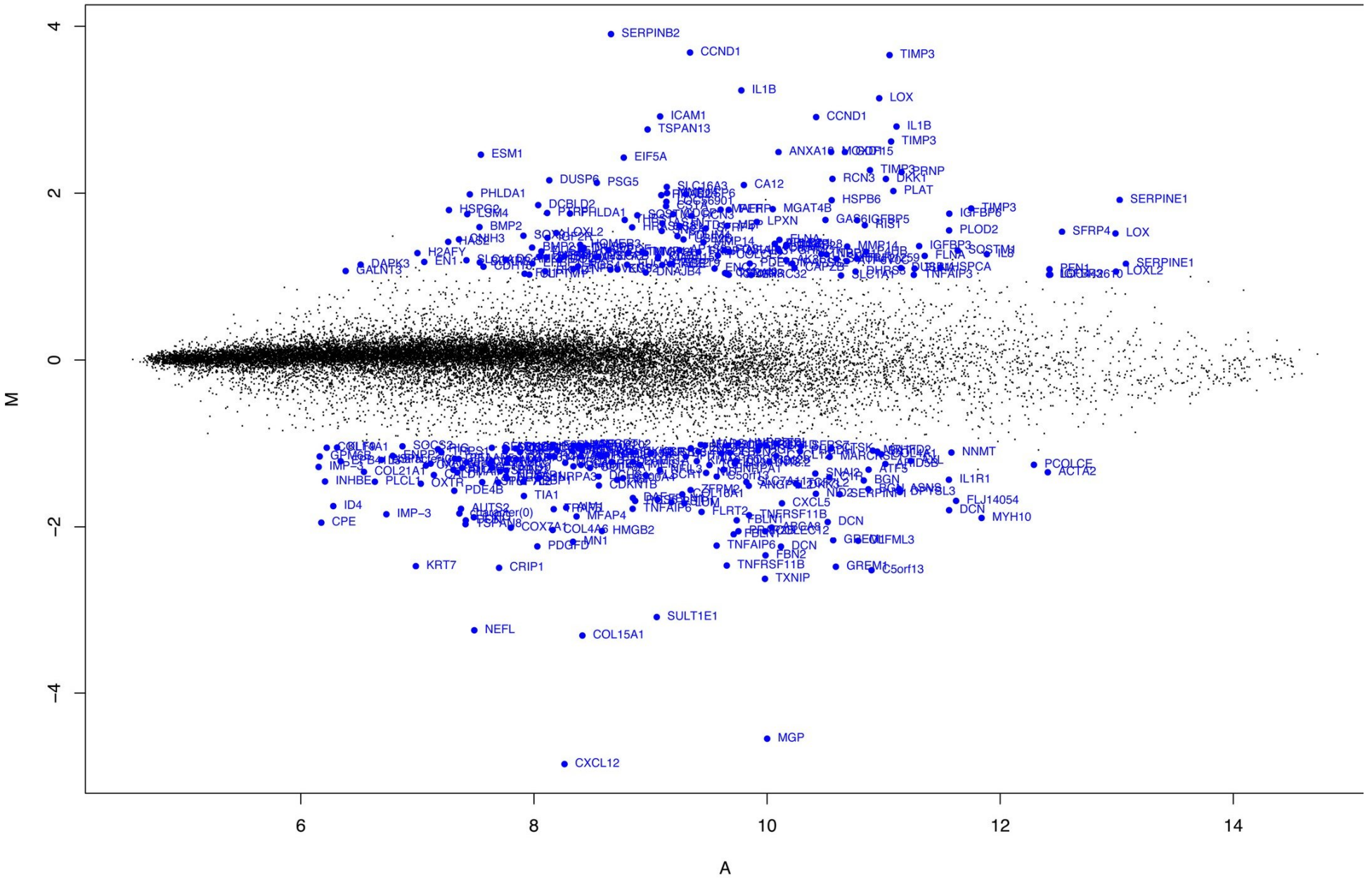

Figure 2: A ratio-intensity plot of the M values (average $\log_2$ fold-change between early and late passage samples, with positive values indicating up-regulation in late passage cells) versus A values (average $\log_2$ expression) for the RMA data. The 327 differentially regulated probesets are given

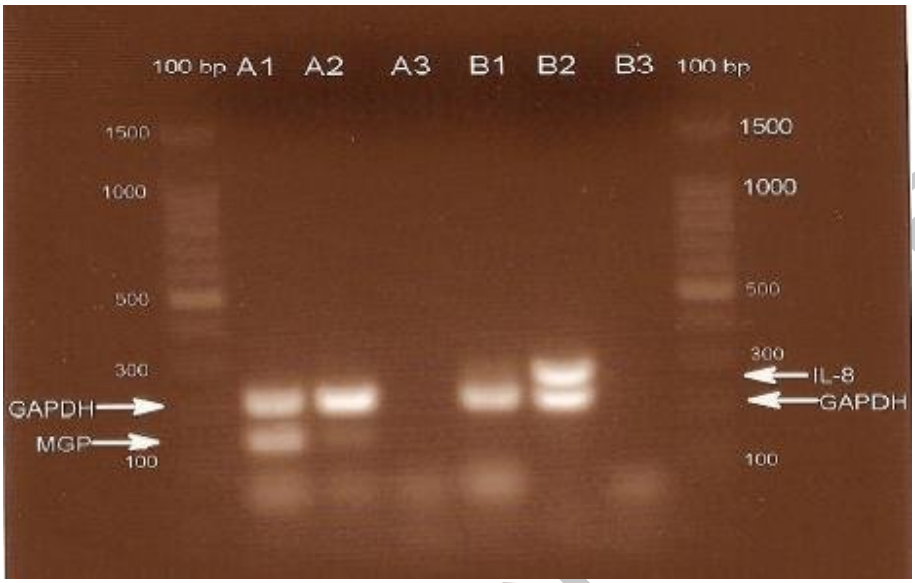

Figure 3: A 1.5% agarose gel photo indicating the presence of the PCR products GAPDH, MGP and IL-8 from early and late passage cDNA samples. Lanes: (A1) early passage, GAPDH and MGP, (A2) late passage, GAPDH and MGP, (A3) negative control, (B1) early passage, GAPDH and IL8, (B2) late passage, GAPDH and IL8, (B3) negative control.

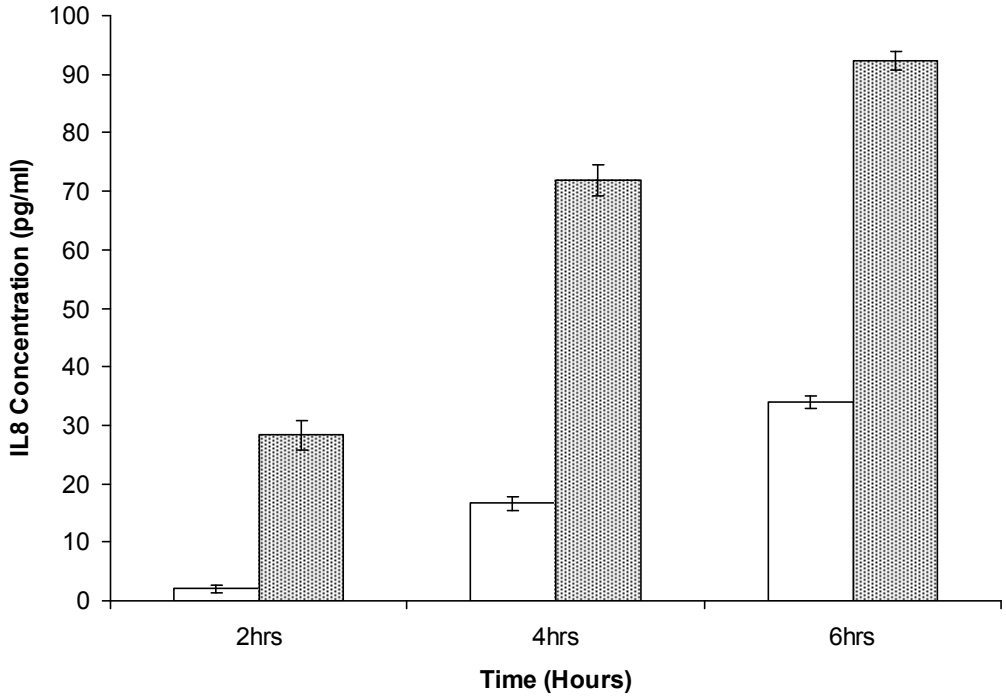

Figure 4: Levels of IL8 in medium obtained from early (14 CPD, white bars) and late (42 CPD, shaded bars) passage cultures of VSMCs collected at 2, 4 and 6 hours after seeding, as determined by ELISA (LPS control data not shown). Data presented as mean ± SD, n=3.

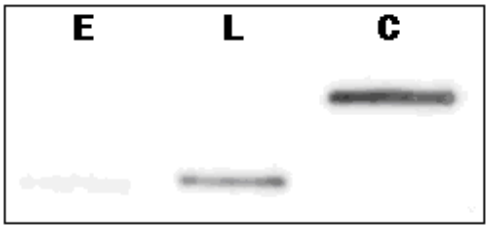

Figure 5: Western blot analysis of IL1β (equal cell numbers). (E) early passage (14 CPD) and (L) late passage (42 CPD) and (C) control (tagged fusion protein)

Affymetrix probeset ID	Gene Symbol	Gene Description	Expression Early (+/- SEM)	Expression Late (+/- SEM)	Fold Change
202291_s_at	MGP	matrix Gla protein	4961 (193.9)	219 (42.3)	23.4
39402_at	IL1B	interleukin 1, beta	290 (28.9)	2816 (581.1)	9.4
202638_s_at	ICAM1	intercellular adhesion molecule 1 (CD54)	208 (43.6)	1493 (54.6)	7.6
205067_at	IL1B	interleukin 1, beta	845 (76.7)	5941 (770.0)	7.0
204933_s_at	TNFRSF11B	osteoprotegerin	1896 (83.0)	344 (17.5)	5.5
208394_x_at	ESM1	endothelial cell-specific molecule 1	81 (8.9)	465 (105.0)	5.5
211896_s_at	DCN	decorin	2420 (124.4)	514 (26.2)	4.7
202827_s_at	MMP14	matrix metallopeptidase 14	283 (11.7)	1143 (124.2)	4.0
211813_x_at	DCN	decorin	2885 (131.1)	774 (131.9)	3.8
209335_at	DCN	decorin	337 (39.5)	89 (10.4)	3.8
211506_s_at	IL8	interleukin 8	560 (135.7)	2131 (559.9)	3.8
204932_at	TNFRSF11B	osteoprotegerin	1778 (215.6)	485 (29.7)	3.6
201893_x_at	DCN	decorin	5644 (156.6)	1631 (133.8)	3.5
205290_s_at	BMP2	bone morphogenetic protein 2	107 (4.8)	346 (82.4)	3.0
217279_x_at	MMP14	matrix metallopeptidase 14	432 (30.5)	1145 (16.5)	2.7
160020_at	MMP14	matrix metallopeptidase 14	1034 (73.2)	2649 (138.8)	2.6
205289_at	BMP2	bone morphogenetic protein 2	159 (3.3)	432 (99.5)	2.5
210513_s_at	VEGF	vascular endothelial growth factor	257 (33.0)	646 (103.4)	2.5
202643_s_at	TNFAIP3	tumor necrosis factor, alpha-induced protein 3	523 (28.5)	1295 (111.8)	2.5
202828_s_at	MMP14	matrix metallopeptidase 14	313 (19.7)	765 (51.7)	2.4
202859_x_at	IL8	interleukin 8	2462 (229.7)	5885 (257.7)	2.4
203683_s_at	VEGFB	vascular endothelial growth factor B	253 (47.4)	579 (27.7)	2.4
211527_x_at	VEGF	vascular endothelial growth factor	278 (17.6)	591 (45.0)	2.1
202637_s_at	ICAM1	intercellular adhesion molecule 1 (CD54)	573 (21.1)	1165 (49.3)	2.0
202644_s_at	TNFAIP3	tumor necrosis factor, alpha-induced protein 3	1721 (16.5)	3563 (481.5)	2.0
202912_at	ADM	adrenomedullin	1124 (42.0)	2316 (550.5)	1.9
216598_s_at	CCL2	chemokine (C-C motif) ligand 2	1671 (241.0)	3103 (258.4)	1.9
215485_s_at	ICAM1	intercellular adhesion molecule 1 (CD54)	211 (9.0)	325 (32.2)	1.5
209875_s_at	SPP1	secreted phosphoprotein 1	56 (1.0)	77 (6.4)	1.4
212171_x_at	VEGF	vascular endothelial growth factor	1417 (77.5)	1708 (179.7)	1.2
210512_s_at	VEGF	vascular endothelial growth factor	4672 (90.1)	4572 (380.3)	1.0

Table 1: Markers associated with atherosclerosis and vascular calcification. Transcript levels (as judged by Affymetrix RMA) are shown for a range of probesets associated with atherosclerosis and vascular calcification from early (14 CPD) and late (39-42 CPD) passage samples. For each probeset, an average expression +/- SEM is shown (n=3). Fold change compares transcript levels in late passage samples with early passage samples. Data sorted based on fold change.